Measurement of CP asymmetry in $D^0 \to K^- K^+$ and $D^0 \to \pi^- \pi^+$ decays

The LHCb collaboration

E-mail: Jeroen.van.Tilburg@cern.ch

ABSTRACT: Time-integrated CP asymmetries in D^0 decays to the final states $K^- K^+$ and $\pi^- \pi^+$ are measured using proton-proton collisions corresponding to $3\,\text{fb}^{-1}$ of integrated luminosity collected at centre-of-mass energies of $7\,\text{TeV}$ and $8\,\text{TeV}$. The D^0 mesons are produced in semileptonic b-hadron decays, where the charge of the accompanying muon is used to determine the initial flavour of the charm meson. The difference in CP asymmetries between the two final states is measured to be

$$\Delta A_{CP} = A_{CP}(K^- K^+) - A_{CP}(\pi^- \pi^+) = (+0.14 \pm 0.16\,(\text{stat}) \pm 0.08\,(\text{syst}))\% .$$

A measurement of $A_{CP}(K^- K^+)$ is obtained assuming negligible CP violation in charm mixing and in Cabibbo-favoured D decays. It is found to be

$$A_{CP}(K^- K^+) = (-0.06 \pm 0.15\,(\text{stat}) \pm 0.10\,(\text{syst}))\%,$$

where the correlation coefficient between ΔA_{CP} and $A_{CP}(K^- K^+)$ is $\rho = 0.28$. By combining these results, the CP asymmetry in the $D^0 \to \pi^- \pi^+$ channel is $A_{CP}(\pi^- \pi^+) = (-0.20 \pm 0.19\,(\text{stat}) \pm 0.10\,(\text{syst}))\%$.

KEYWORDS: CP violation, Charm physics, Flavor physics, Hadron-Hadron Scattering

ARXIV EPRINT: 1405.2797

Contents

1 Introduction

Decays of charm mesons mediated by the weak interaction provide an attractive testing ground for physics beyond the Standard Model (SM). Violations of charge-parity (CP) symmetry are predicted to be small in charm decays, but could be enhanced in the presence of non-SM physics. Direct CP violation arises when two or more amplitudes with different weak and strong phases contribute to the same final state. This is possible in singly Cabibbo-suppressed $D^0 \to K^- K^+$ and $D^0 \to \pi^- \pi^+$ decays,[1] where significant penguin contributions can be expected [1]. Under SU(3) flavour symmetry, which is approximately valid in heavy quark transitions, the direct CP asymmetries in these decays are expected to have equal magnitudes and opposite sign. For a long time, direct CP violation in these decays was expected to be below the 10^{-3} level [2]; however, this prediction has been revisited recently and asymmetries at a few times 10^{-3} cannot be excluded within the

---

[1]The inclusion of charge-conjugate processes is implied throughout this paper, unless explicitly stated otherwise.

SM [3–6]. Indirect CP violation, occurring through D^0 mixing, is expected to be negligible at the current experimental precision [2, 7] and measured to be consistent with zero [8]. To date, CP violation in charm decays has not been established experimentally.

In this paper the CP asymmetries in $D^0 \to K^- K^+$ and $D^0 \to \pi^- \pi^+$ decays are measured in semileptonic b-hadron decays using the muon charge to identify (tag) the flavour of the D^0 meson at production. This time-integrated CP asymmetry receives contributions from both direct and indirect CP violation. The difference of these asymmetries (ΔA_{CP}) was measured at LHCb [9–11]. Assuming indirect CP violation to be independent of the decay mode [2, 7], only the effect of direct CP violation remains in ΔA_{CP}. This paper supersedes the previous ΔA_{CP} result from ref. [11] that was based on one third of the data. In this paper the individual CP asymmetries in $D^0 \to \pi^- \pi^+$ and $D^0 \to K^- K^+$ decays are also measured, using samples of Cabibbo-favoured D^0 and D^+ decays to correct for spurious asymmetries due to detection and production effects. Individual CP asymmetries and their difference have been measured by several other experiments [12–16], all using D^0 mesons tagged by the charge of the pion from $D^{*+} \to D^0 \pi^+$ decays. The world average values [8] are $A_{CP}(K^- K^+) = (-0.15 \pm 0.14)\%$ and $A_{CP}(\pi^- \pi^+) = (0.18 \pm 0.15)\%$ for the individual asymmetries and $\Delta A_{CP} = (-0.33 \pm 0.12)\%$ for the difference.

2 Method and formalism

Our procedure to measure the difference in CP asymmetries, ΔA_{CP}, follows ref. [11]. The observed (raw) asymmetry for a D meson decay rate to a final state f is defined as

$$A_{\text{raw}} \equiv \frac{N(D \to f) - N(\overline{D} \to \overline{f})}{N(D \to f) + N(\overline{D} \to \overline{f})}, \qquad (2.1)$$

where N is the number of observed decays, D is either a D^+ or D^0 meson, and $\overline{D}$ is either a D^- or $\overline{D}^0$ meson. For decays to a CP eigenstate, where $f = \overline{f}$, the initial flavour of the D^0 meson is tagged by the charge of the accompanying muon in the semileptonic decay $\overline{B} \to D^0 \mu^- \overline{\nu}_\mu X$, where X denotes possible other particles produced in the decay. Neglecting third-order terms in the asymmetries, the raw asymmetry in the decays $D^0 \to K^- K^+$ and $D^0 \to \pi^- \pi^+$ is

$$A_{\text{raw}} = A_{CP} + A_D(\mu^-) + A_P(\overline{B}), \qquad (2.2)$$

where $A_D(\mu^-)$ is any charge-dependent asymmetry in muon reconstruction efficiency and $A_P(\overline{B})$ is the asymmetry between the numbers of b and $\bar{b}$ hadrons (denoted as $\overline{B}$ and B, respectively) produced in the LHCb acceptance, which includes possible CP violation in B^0 mixing. The production and detection asymmetries are common to the $D^0 \to K^- K^+$ and $D^0 \to \pi^- \pi^+$ decay modes, so they cancel in the difference of the raw asymmetries, giving

$$\Delta A_{CP} = A_{\text{raw}}(K^- K^+) - A_{\text{raw}}(\pi^- \pi^+) = A_{CP}(K^- K^+) - A_{CP}(\pi^- \pi^+). \qquad (2.3)$$

The production and muon detection asymmetry in eq. (2.2) can also be removed using the Cabibbo-favoured $D^0 \to K^- \pi^+$ decay mode in $\overline{B} \to D^0 \mu^- \overline{\nu}_\mu X$ decays. In this decay, CP violation can be neglected as it is expected to be significantly suppressed compared to

our sensitivity for measuring CP violation in $D^0 \to K^-K^+$ and $D^0 \to \pi^-\pi^+$ decays. In the reconstruction of the $K^-\pi^+$ final state there is an instrumental asymmetry, $A_D(K^-\pi^+)$, due to the different interaction cross section of positively and negatively charged kaons in the detector material. Also, other detector-related effects, for example due to the acceptance, selection and detection inefficiencies, can contribute to this detection asymmetry. The raw asymmetry in this decay mode is then

$$A_{\mathrm{raw}}(K^-\pi^+) = A_D(\mu^-) + A_P(\overline{B}) + A_D(K^-\pi^+) \,. \tag{2.4}$$

The detection asymmetry $A_D(K^-\pi^+)$ of the final state $K^-\pi^+$ is obtained from D^+ decays produced directly in pp collisions (so-called *prompt* D^+ decays). Two decay modes are used, $D^+ \to K^-\pi^+\pi^+$ and $D^+ \to \overline{K}^0\pi^+$ with $\overline{K}^0 \to \pi^+\pi^-$. The raw asymmetry of $D^+ \to K^-\pi^+\pi^+$ decays is

$$A_{\mathrm{raw}}(K^-\pi^+\pi^+) = A_P(D^+) + A_D(K^-\pi^+) + A_D(\pi^+)\,, \tag{2.5}$$

where $A_P(D^+)$ is the production asymmetry of prompt D^+ mesons and $A_D(\pi^+)$ is the detection asymmetry of the other charged pion. The raw asymmetry of $D^+ \to \overline{K}^0\pi^+$ decays is

$$A_{\mathrm{raw}}(\overline{K}^0\pi^+) = A_P(D^+) + A_D(\pi^+) - A_D(K^0)\,, \tag{2.6}$$

where $A_D(K^0)$ is the detection asymmetry of the decay $K^0 \to \pi^+\pi^-$, which is discussed later. Taking the difference between eqs. (2.5) and (2.6), $A_D(K^-\pi^+)$ is obtained as

$$A_D(K^-\pi^+) = A_{\mathrm{raw}}(K^-\pi^+\pi^+) - A_{\mathrm{raw}}(\overline{K}^0\pi^+) - A_D(K^0) \,. \tag{2.7}$$

This method assumes negligible CP violation in these Cabibbo-favoured D^+ decay modes. By combining eqs. (2.2) and (2.4), the CP asymmetry in the $D^0 \to K^-K^+$ decay becomes

$$A_{CP}(K^-K^+) = A_{\mathrm{raw}}(K^-K^+) - A_{\mathrm{raw}}(K^-\pi^+) + A_D(K^-\pi^+)\,, \tag{2.8}$$

where $A_D(K^-\pi^+)$ is taken from eq. (2.7). The CP asymmetry in the $D^0 \to \pi^-\pi^+$ decay is determined from the difference between the measurements of $A_{CP}(K^-K^+)$ and ΔA_{CP}.

3 Detector

The LHCb detector [17] is a single-arm forward spectrometer covering the pseudorapidity range $2 < \eta < 5$, designed for the study of particles containing b or c quarks. The detector includes a high-precision tracking system consisting of a silicon-strip vertex detector surrounding the pp interaction region, a large-area silicon-strip detector located upstream of a dipole magnet with a bending power of about $4\,\mathrm{Tm}$, and three stations of silicon-strip detectors and straw drift tubes placed downstream of the magnet. The polarity of the magnetic field is regularly reversed during data taking. The combined tracking system provides a momentum measurement with relative uncertainty that varies from 0.4% at low momentum, p, to 0.6% at $100\,\mathrm{GeV}/c$, and impact parameter resolution of $20\,\mu\mathrm{m}$ for charged particles with large transverse momentum, p_{T}. Different types of charged hadrons

are distinguished by information from two ring-imaging Cherenkov detectors [18]. Photon, electron and hadron candidates are identified by a calorimeter system consisting of scintillating-pad and preshower detectors, an electromagnetic calorimeter and a hadronic calorimeter. Muons are identified by a system composed of alternating layers of iron and multiwire proportional chambers. The trigger [19] consists of a hardware stage, based on information from the calorimeter and muon systems, followed by a two-stage software stage, that applies a full event reconstruction.

4 Data set and selection

This analysis uses the data set collected by LHCb corresponding to an integrated luminosity of $3\,\text{fb}^{-1}$. The data in 2011 ($1\,\text{fb}^{-1}$) were taken at a centre-of-mass energy of 7TeV and the data in 2012 ($2\,\text{fb}^{-1}$) were taken at a centre-of-mass energy of 8TeV. The fraction of data collected with up (down) polarity of the magnetic field is 40% (60%) in 2011 and 52% (48%) in 2012. Charge-dependent detection asymmetries originating from any left-right asymmetry in the detector change sign when the field polarity is reversed. By design, the analysis method does not rely on any cancellation due to the regular field reversals, since all detection asymmetries are already removed in the determination of the CP asymmetries. This assumption is tested by performing the analysis separately for the two polarities. To ensure that any residual detection asymmetries cancel, the raw asymmetries are determined from the arithmetic mean of the results obtained for the two magnet polarities. Similarly, the analysis is performed separately for the 2011 and 2012 data as detection asymmetries and production asymmetries change due to different operational conditions.

At the hardware trigger stage, the events in the semileptonic B decay modes are required to be triggered by the muon system. The muon transverse momentum must be larger than $1.64\,\text{GeV}/c$ for the 2011 data and larger than $1.76\,\text{GeV}/c$ for the 2012 data. In the software trigger, the muon candidate is first required to have $p_\text{T} > 1.0\,\text{GeV}/c$ and a large impact parameter. Then, the muon and one or two of the D^0 decay products are required to be consistent with the topological signature of b-hadron decays [19]. Since the ΔA_{CP} measurement has no detection asymmetry coming from the D^0 decay products, B candidates triggered on the presence of a final-state particle with high p_T and large impact parameter are also accepted in the corresponding selection.

The remaining selection of semileptonic B decays reduces the background from prompt D^0 decays to the per-cent level. The residual background consists mainly of combinations from inclusive b-hadron decays with other particles in the event. The selection is similar to that in the previous publication [11], except for the looser particle identification requirements of the kaon candidates. To reduce the large $D^0 \to K^-\pi^+$ sample size only half of the candidates (randomly selected) is kept.

In order to reduce possible biases induced by trigger criteria, the events in the prompt charm decay modes are selected by the hardware trigger, independently of the presence of the D^+ candidate. In the software trigger, one of the final-state pions is first required to have $p_\text{T} > 1.6\,\text{GeV}/c$ and a large impact parameter to any primary vertex. This ensures that the distributions of the kaon and the other pion in the $D^+ \to K^-\pi^+\pi^+$ decay and of the

$\overline{K}^0$ meson in the $D^+ \to \overline{K}^0 \pi^+$ decay are not biased by these trigger requirements. Finally, an exclusive selection is applied for each D^+ decay mode in the last stage of the software trigger. This is similar to the offline selection, where a secondary vertex is reconstructed and required to be significantly displaced from any primary vertex.

All particles are required to have $p > 2\,\mathrm{GeV}/c$ and $p_\mathrm{T} > 250\,\mathrm{MeV}/c$. Additionally, all tracks in the $D^+ \to K^- \pi^+ \pi^+$ and $D^+ \to \overline{K}^0 \pi^+$ decays are required to have a large impact parameter with respect to any primary vertex. The particle identification requirements are the same as those in the $D^0 \to K^- \pi^+$ decay mode from semileptonic B decays. The neutral kaon in the $D^+ \to \overline{K}^0 \pi^+$ decay is detected in the $\pi^+ \pi^-$ final state, which is dominated by the decay of the K_S^0 state. When K_S^0 mesons decay early such that both pions leave sufficiently many hits in the vertex detector and in the three downstream tracking stations, the pions can be reconstructed as so-called *long* tracks. When K_S^0 mesons decay later such that both pions do not leave enough hits in the vertex detector, but enough hits in the rest of the tracking system, the pions can be reconstructed as so-called *downstream* tracks. Downstream K_S^0 candidates are available only in 2012 data, since no dedicated trigger was available to select these decays in 2011. For this reason, only $D^+ \to \overline{K}^0 \pi^+$ decays formed with long K_S^0 candidates are used for the asymmetry measurement. The downstream K_S^0 candidates are used to check the effect of the K^0 detection asymmetry. There is no p_T requirement for the pions from downstream K_S^0 candidates. All K_S^0 candidates are required to have a large impact parameter. Both D^+ and K_S^0 candidates are required to have $p_\mathrm{T} > 1\,\mathrm{GeV}/c$ and an accurately reconstructed decay vertex. For the $D^+ \to K^- \pi^+ \pi^+$ decay the scalar p_T sum of the D^+ daughters is required to be larger than $2.8\,\mathrm{GeV}/c$. The D^+ candidates should have a large impact parameter and significant flight distance from the primary vertex. Given the large branching fraction of the $D^+ \to K^- \pi^+ \pi^+$ decay, only one fifth of the available data set (randomly selected) is considered in the following.

To improve the mass resolution, a vertex fit [20] of the D^+ decay products is made, where the D^+ candidate is constrained to originate from the corresponding primary vertex. Additionally, in the decay $D^+ \to \overline{K}^0 \pi^+$ the mass of the $\overline{K}^0$ meson is constrained to the nominal value [21]. The momentum of all particles is corrected [22] to improve the stability of the mass scale versus data taking period and to reduce the width of the mass distribution.

5 Determination of the asymmetries

In this section the raw asymmetries are obtained from fits to the invariant mass distributions. These numbers are corrected for effects coming from the K^0 detection asymmetry and wrong flavour tags. The contributions from direct and indirect CP violation are determined and finally the CP asymmetries are calculated.

5.1 Invariant mass distributions

Invariant mass distributions for the D^0 and D^+ candidates are shown in figure 1 with the fit results overlaid. For all decay modes the signal is modelled by the sum of two Gaussian functions with common mean and a power-law tail. For decays to non-CP eigenstates (i.e., $D^0 \to K^- \pi^+$, $D^+ \to K^- \pi^+ \pi^+$, $D^+ \to \overline{K}^0 \pi^+$) different means and average widths are

Decay sample	Signal decays
$D^0 \to \pi^- \pi^+$ from B	773 541
$D^0 \to K^- K^+$ from B, ΔA_{CP} selection	2 166 045
$D^0 \to K^- K^+$ from B, $A_{CP}(K^- K^+)$ selection	1 821 462
$D^0 \to K^- \pi^+$ from B	9 088 675
Prompt $D^+ \to K^- \pi^+ \pi^+$	40 782 645
Prompt $D^+ \to \overline{K}^0 \pi^+$, long K^0_S	3 765 530
Prompt $D^+ \to \overline{K}^0 \pi^+$, downstream K^0_S	2 512 615

Table 1. Number of signal decays determined from fits to the invariant mass distributions.

allowed between D and $\overline{D}$ states, due to a known charge-dependent bias in the measurement of the momentum. The background is described by an exponential function, with different slopes for D and $\overline{D}$ states. An overall asymmetry in the number of background events is also included in the model. The background from misidentified $D^0 \to K^- \pi^+$ decays in the $D^0 \to \pi^- \pi^+$ invariant mass distribution is modelled with a single Gaussian function with the same shape for both muon tags and an additional asymmetry parameter. The numbers of signal decays determined from fits to the invariant mass distributions are given in table 1.

5.2 Differences in kinematic distributions

Production and detection asymmetries depend on the kinematic distributions of the particles involved. Since the momentum distributions of the particles in the signal and calibration decay modes are different, small residual production and detection asymmetries can remain in the calculation of ΔA_{CP} and $A_{CP}(K^- K^+)$. This effect is mitigated by assigning weights to each candidate such that the kinematic distributions are equalised. For the measurement of ΔA_{CP}, the $D^0 \to K^- K^+$ candidates are weighted according to the p_{T} and η values of the D^0, which are the kinematic variables showing the most significant differences. The weights are chosen such that the weighted and background-subtracted distributions of the D^0 and muon candidates agree with the corresponding (unweighted) distributions in the $D^0 \to \pi^- \pi^+$ sample. After weighting, the effective sample size is given by $N_{\mathrm{eff}} = (\sum_{i=1}^{N} w_i)^2 / (\sum_{i=1}^{N} w_i^2)$, where w_i is the weight of candidate i and N the total number of candidates. Due to the good agreement in the kinematic distributions between the two decays, this procedure reduces the statistical power of the weighted $D^0 \to K^- K^+$ event sample by only 8%.

For the measurement of $A_{CP}(K^- K^+)$, additional weighting steps for the D^+ calibration decay modes are needed. In the first step, the $D^0 \to K^- \pi^+$ candidates are weighted based on the p_{T} and η values of the D^0 meson, such that they agree with the corresponding (unweighted) distributions of the $D^0 \to K^- K^+$ candidates. This step, which reduces the statistical power of the $D^0 \to K^- \pi^+$ sample by 3%, ensures the cancellation of the B production asymmetry and muon detection asymmetry. In the second step, the
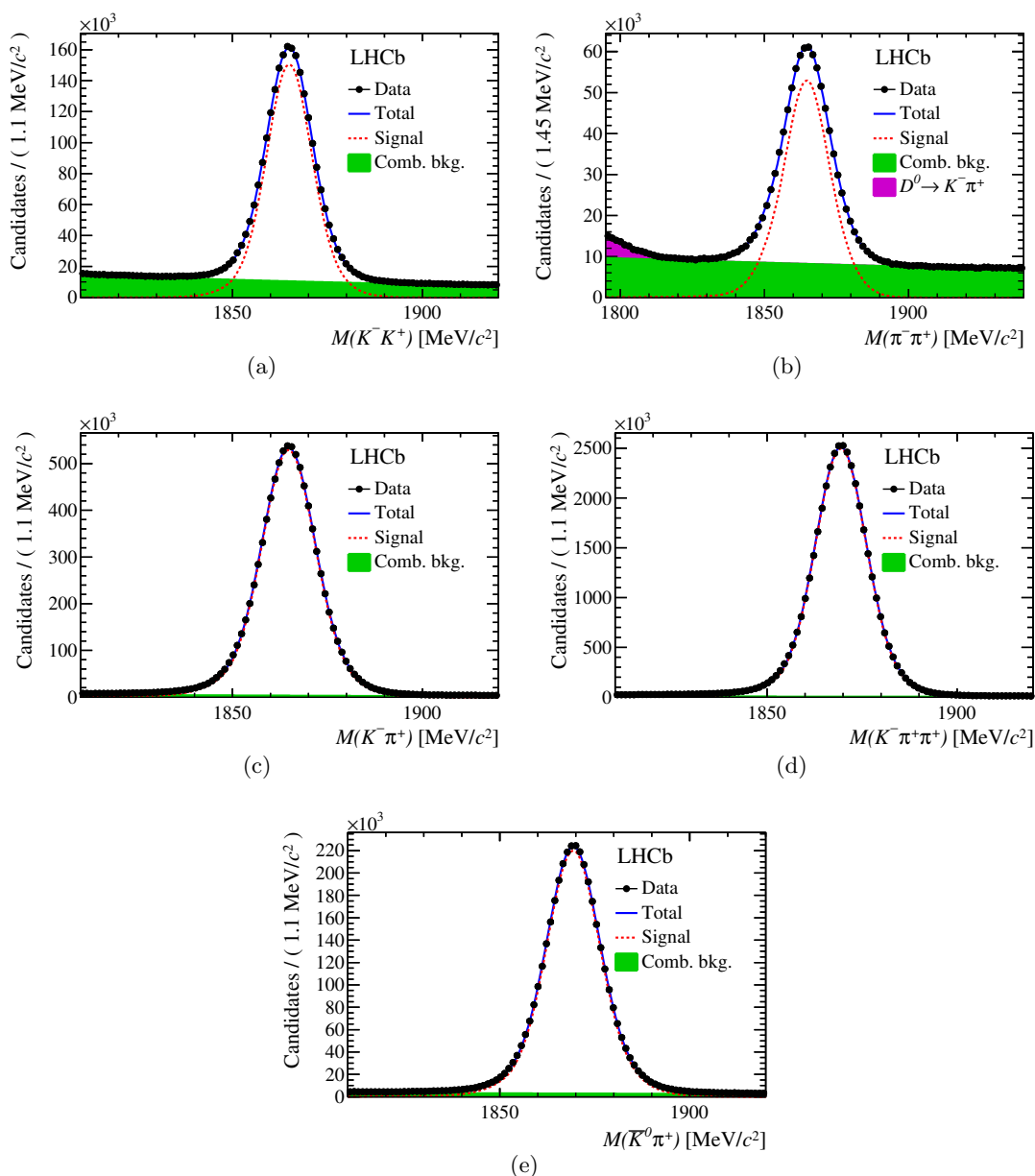
Figure 1. Invariant mass distributions for muon-tagged (a) $D^0 \to K^- K^+$, (b) $D^0 \to \pi^- \pi^+$ and (c) $D^0 \to K^- \pi^+$ candidates and for prompt (d) $D^+ \to K^- \pi^+ \pi^+$ and (e) $D^+ \to \overline{K}^0 \pi^+$ candidates. The results of the fits are overlaid.

$D^+ \to K^- \pi^+ \pi^+$ candidates are weighted according to the p_{T} and η values of both the kaon and the pion that was not selected by the software trigger. This step equalises the kinematic distributions of the K^- and π^+ to those of the (now weighted) $D^0 \to K^- \pi^+$ decay to ensure cancellation of the $K^- \pi^+$ detection asymmetry. The resulting 50% reduction in statistical power does not contribute to the final uncertainty given the large number of $D^+ \to K^- \pi^+ \pi^+$ candidates available. In the last step, the $D^+ \to \overline{K}^0 \pi^+$ candidates are weighted according to the p_{T} and η values of both the pion and the D^+ candidate, such that

they agree with the corresponding (weighted) distributions of the $D^+ \to K^-\pi^+\pi^+$ candidates. The last step ensures cancellation of the D^+ production asymmetry and detection asymmetry from the pion that is used in the software trigger and reduces the statistical power of the $D^+ \to \overline{K}^0\pi^+$ sample by 77%.

5.3 K^0 asymmetry

An asymmetry in the detection of a K^0 to the $\pi^+\pi^-$ final state arises from the combined effect of CP violation and mixing in the neutral kaon system and the different interaction rates of K^0 and $\overline{K}^0$ in the detector material. Due to material interactions, a pure K^0_L state can change back into a superposition of K^0_L and K^0_S states [23]. These regeneration and CP-violating effects are of the same order and same sign in LHCb. To estimate the total K^0 detection asymmetry, the mixing, CP violation and absorption in material need to be described coherently. The amplitudes in the K^0_L and K^0_S basis of an arbitrary neutral kaon state in matter evolve as [24]

$$\alpha_{\rm L}(t) = {\rm e}^{-i\,t\,\Sigma}\left[\alpha_{\rm L}(0)\cos\left(\Omega t\right) - i\frac{\alpha_{\rm L}(0)\Delta\lambda + \alpha_{\rm S}(0)\Delta\chi}{2\Omega}\sin\left(\Omega t\right)\right], \qquad (5.1)$$

$$\alpha_{\rm S}(t) = {\rm e}^{-i\,t\,\Sigma}\left[\alpha_{\rm S}(0)\cos\left(\Omega t\right) + i\frac{\alpha_{\rm S}(0)\Delta\lambda - \alpha_{\rm L}(0)\Delta\chi}{2\Omega}\sin\left(\Omega t\right)\right], \qquad (5.2)$$

where the constants $\Omega \equiv \frac{1}{2}\sqrt{\Delta\lambda^2 + \Delta\chi^2}$ and $\Sigma \equiv \frac{1}{2}(\lambda_{\rm L} + \lambda_{\rm S} + \chi + \bar{\chi})$ are given by the masses $m_{\rm L,S}$ and decay widths $\Gamma_{\rm L,S}$ of the K^0_L and K^0_S states and by the absorption χ $(\bar{\chi})$ of K^0 $(\overline{K}^0)$ states through

$$\Delta\lambda = \lambda_{\rm L} - \lambda_{\rm S} = \Delta m - \frac{i}{2}\Delta\Gamma = (m_{\rm L} - m_{\rm S}) - \frac{i}{2}(\Gamma_{\rm L} - \Gamma_{\rm S}),$$

$$\Delta\chi = \chi - \bar{\chi} = -\frac{2\pi\mathcal{N}}{m}(f - \bar{f}) = -\frac{2\pi\mathcal{N}}{m}\Delta f, \qquad (5.3)$$

where $\mathcal{N}$ is the scattering density, m the kaon mass, and f and $\bar{f}$ the forward scattering amplitudes. The imaginary part of f is related to the total cross section through the optical theorem $\sigma_T = (4\pi/p){\rm Im}f$. The difference in the interaction cross sections of $\overline{K}^0$ and K^0 depends on the momentum of the kaon and on the number of nucleons, A, in the target and is obtained from ref. [25],

$$\Delta\sigma = \sigma_T(\overline{K}^0) - \sigma_T(K^0) = 23.2\,A^{0.758}[p({\rm GeV}/c)]^{-0.614}\,{\rm mb}\ . \qquad (5.4)$$

The phase of Δf is determined using the phase-power relation [25, 26] to be $\arg(\Delta f) = (-124.7 \pm 0.8)°$. The regeneration incorporates two effects [23, 27]. The term ${\rm Im}(\Delta f)$ describes the incoherent regeneration due to absorption and elastic scattering, which is equivalent to the case of charged kaons. The term ${\rm Re}(\Delta f)$ describes the coherent regeneration due to dispersion (phase shift) of the K^0 and $\overline{K}^0$ states.

As the neutral kaons are produced in a flavour eigenstate, the initial amplitudes at $t = 0$, $\alpha_{\rm L,S}(0)$, need to be written in the K^0_L and K^0_S basis,

$$|K^0\rangle, |\overline{K}^0\rangle = \sqrt{\frac{1 + |\epsilon|^2}{2}}\frac{1}{1 \pm \epsilon}\left[|K^0_L\rangle \pm |K^0_S\rangle\right], \qquad (5.5)$$

– 8 –

Parameter	Value
Δm	$(0.5293 \pm 0.0009) \times 10^{10} \hbar\,\mathrm{s}^{-1}$
$\tau_{\mathrm{S}} \equiv 1/\Gamma_{\mathrm{S}}$	$(0.8954 \pm 0.0004) \times 10^{-10}\,\mathrm{s}$
$\tau_{\mathrm{L}} \equiv 1/\Gamma_{\mathrm{L}}$	$(5.116 \pm 0.021) \times 10^{-8}\,\mathrm{s}$
m	$(497.614 \pm 0.024)\,\mathrm{MeV}/c^2$
$\arg(\Delta f)$	$(-124.7 \pm 0.8)^\circ$
$|\epsilon|$	$(2.228 \pm 0.011) \times 10^{-3}$
$\phi_{+-} \equiv \arg \epsilon$	$(43.51 \pm 0.05)^\circ$

Table 2. Values of the parameters used to calculate the K^0 asymmetry [21, 25].

where ϵ describes CP violation in kaon mixing. At a given time, the decay rate into the final state $\pi^+\pi^-$ is given by $|\alpha_{\mathrm{S}}(t) + \epsilon\,\alpha_{\mathrm{L}}(t)|^2$. The values of the parameters used to calculate the K^0 asymmetry are given in table 2.

Using the K^0_{S} and D^0 decay positions, the path of the K^0_{S} meson through the detector is known and the expected K^0 asymmetry can be calculated using the formulae above. For every $D^+ \to \overline{K}^0\pi^+$ candidate, the path of the neutral kaon is divided into small steps using the material model of the LHCb detector. At each step, the amplitudes are updated using eq. (5.2) starting with either a K^0 or $\overline{K}^0$ as initial state. The expected K^0 asymmetry for a given event is then the asymmetry in the decay rates between the K^0 and $\overline{K}^0$ initial states. The overall asymmetry is calculated from the expected asymmetry averaged over all reconstructed $D^+ \to \overline{K}^0\pi^+$ candidates.

The measured raw asymmetry in the $D^+ \to \overline{K}^0\pi^+$ decay and the effect from the predicted K^0 asymmetry are shown as functions of the K^0_{S} decay time in figure 2. The measured raw asymmetry receives contributions not only from the K^0 detection asymmetry, but also from the pion tracking asymmetry and D^+ production asymmetry. These contributions are almost independent of the K^0_{S} decay time. Therefore, an overall shift is applied to the predicted asymmetry to match the data. Assuming a negligible pion detection asymmetry, this shift agrees well with the D^+ production asymmetry of $(-0.96 \pm 0.26)\%$ measured on 2011 data [28]. The downward trend coming from the K^0 asymmetry is clearly visible, in particular for downstream K^0_{S} decays. The predicted asymmetry dependence agrees well with the data, with p-values of 0.81 and 0.31, respectively.

Only K^0_{S} candidates reconstructed with long tracks are used in the $A_{CP}(K^-K^+)$ measurement. These candidates probe lower K^0_{S} decay times, compared to those reconstructed with downstream tracks, resulting in a much smaller K^0 asymmetry correction. Nevertheless, the effect observed in downstream K^0_{S} decays is used to test the accuracy of the K^0 detection asymmetry model. The measured difference in raw asymmetry between the samples is $(0.49 \pm 0.12)\%$, which is obtained after weighting the long K^0_{S} sample to correct for differences in the D^+ production and pion detection asymmetries. This value agrees with the expected difference of $(0.546 \pm 0.027)\%$, where the uncertainty is dominated by the uncertainty on the amount of detector material. The relative uncertainty of
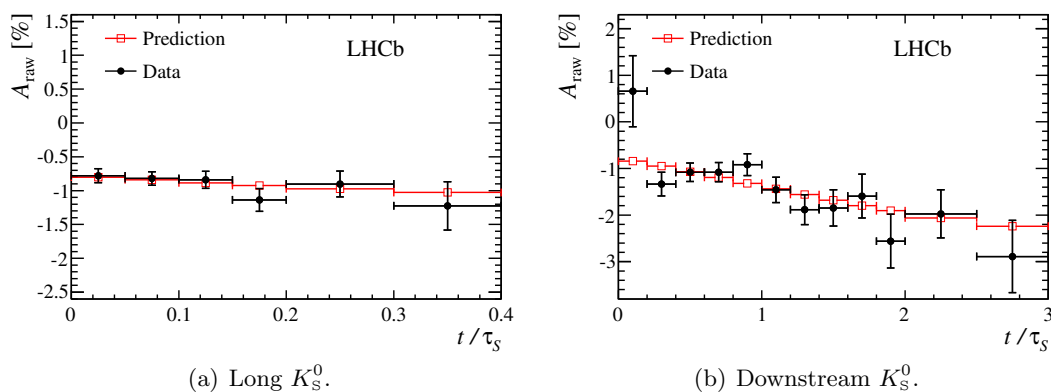
Figure 2. Raw asymmetry in the $D^+ \to \overline{K}^0 \pi^+$ decay shown for (a) long and (b) downstream K_S^0 candidates versus the K_S^0 decay time in units of its lifetime. The long K_S^0 candidates are reconstructed in the full data set, while the downstream K_S^0 candidates are reconstructed in the 2012 data only. The predicted effect from the K^0 asymmetry, $-A_D(K^0)$, is also shown. An overall shift is applied to this prediction to account for D^+ production and pion detection asymmetries (note that the unshifted $A_D(K^0)$ at $t = 0$ is zero).

the measured difference (25%) is assigned as a systematic uncertainty on the K^0 asymmetry model. The expected K^0 asymmetry in the $D^+ \to \overline{K}^0 \pi^+$ sample with long K_S^0 candidates weighted according to the procedure described in section 5.2 is found to be $A_D(K^0) = (0.054 \pm 0.014\,(\mathrm{syst}))\%$.

5.4 Wrong flavour tags

If a D^0 meson is combined with a muon that does not originate from the corresponding semileptonic B decay, the D^0 flavour may not be correctly assigned. The probability to wrongly tag a D^0 meson is denoted by ω. This mistag probability dilutes the observed asymmetry by a factor $1 - 2\omega$. For small ω, the expression of ΔA_{CP} can be written as

$$\Delta A_{CP} = (1 + 2\omega)[A_{\mathrm{raw}}(K^-K^+) - A_{\mathrm{raw}}(\pi^-\pi^+)] \,. \tag{5.6}$$

The mistag probability only affects the semileptonic decay modes as the flavour of the D^+ reconstruction is unambiguous. In the reconstruction of the $D^0 \to K^-\pi^+$ decay, wrong-sign decays coming from doubly Cabibbo-suppressed $D^0 \to K^+\pi^-$ decays and mixed $D^0 \to \overline{D}^0 \to K^+\pi^-$ decays are included. Hence, the calculation of the CP asymmetry of the $D^0 \to K^-K^+$ decay is

$$A_{CP}(K^-K^+) = (1 + 2\omega)[A_{\mathrm{raw}}(K^-K^+) - A_{\mathrm{raw}}(K^-\pi^+)] + (1 - 2R)A_D(K^-\pi^+), \tag{5.7}$$

where R is the ratio of branching fractions of wrong-sign $D^0 \to K^+\pi^-$ decays over right-sign $D^0 \to K^-\pi^+$ decays.

The $D^0 \to K^-\pi^+$ sample from semileptonic B decays is also used to estimate the mistag probability. The final state, either $K^+\pi^-$ or $K^-\pi^+$, almost unambiguously determines the flavour of the D^0 meson, since the contamination from wrong-sign decays is only $R =$

$(0.389 \pm 0.003)\%$ [29]. After correcting for this wrong-sign fraction, the mistag probability is found to be $\omega = (0.988 \pm 0.006)\%$ for the ΔA_{CP} measurement and $\omega = (0.791 \pm 0.006)\%$ for the $A_{CP}(K^-K^+)$ measurement. The small difference between these numbers is due to more stringent trigger criteria in the latter, resulting in different kinematic distributions for the two selections. As a consistency check, the mistag probability is obtained in all three semileptonic samples by searching for an additional pion from a $D^{*+} \to D^0\pi^+$ decay and comparing the charge of this pion with that of the muon. The mistag probabilities are found to be in good agreement with an average value of $\omega = (0.985 \pm 0.017)\%$ for the ΔA_{CP} measurement and of $\omega = (0.803 \pm 0.019)\%$ for the $A_{CP}(K^-K^+)$ measurement. Since the dilution effect from such a small ω value results in tiny corrections to ΔA_{CP} and $A_{CP}(K^-K^+)$, the uncertainty in this number is neglected. A small difference of $\Delta\omega = (0.028 \pm 0.011)\%$ is observed between the probabilities to wrongly tag D^0 and $\bar{D}^0$ mesons. Although any non-zero value is expected to cancel in the calculation of ΔA_{CP} and $A_{CP}(K^-K^+)$, the full difference is conservatively taken as a systematic uncertainty.

5.5 Average decay times

The time-integrated CP asymmetry has contributions from direct and indirect CP violation, depending on the average decay time, $\langle t \rangle$, of the D^0 mesons in the sample as [2]

$$A_{CP} \approx a_{CP}^{\mathrm{dir}} - A_\Gamma \frac{\langle t \rangle}{\tau}\,, \tag{5.8}$$

where a_{CP}^{dir} is the direct CP violation term, τ the D^0 lifetime, and A_Γ a measure of indirect CP violation. The world-average value of A_Γ in singly Cabibbo-suppressed D^0 decays is $(-0.014 \pm 0.052)\%$ [8]. Assuming that this quantity is the same for $D^0 \to K^-K^+$ and $D^0 \to \pi^-\pi^+$ decays, the sensitivity of ΔA_{CP} to indirect CP violation is introduced by the difference in the average D^0 decay times between the two decay modes. A complete discussion is given in the previous publication [11] and the same procedure is adopted here. In this procedure, the average decay time of the signal in each sample is determined by subtracting the decay time distributions of background events using the *sPlot* technique [30], and by correcting for decay time resolution effects. For the ΔA_{CP} measurement, the average decay times are found to be

$$\langle t \rangle / \tau (K^-K^+) = 1.082 \pm 0.001\,(\mathrm{stat}) \pm 0.004\,(\mathrm{syst})\,,$$
$$\langle t \rangle / \tau (\pi^-\pi^+) = 1.068 \pm 0.001\,(\mathrm{stat}) \pm 0.004\,(\mathrm{syst})\,.$$

The small difference between these numbers (0.014 ± 0.004) implies that $\Delta A_{CP} = \Delta a_{CP}^{\mathrm{dir}}$ is an excellent approximation. For the $A_{CP}(K^-K^+)$ measurement, the average decay time is found to be

$$\langle t \rangle / \tau (K^-K^+) = 1.051 \pm 0.001\,(\mathrm{stat}) \pm 0.004\,(\mathrm{syst})\,.$$

5.6 CP asymmetry measurements

The raw asymmetries are determined with likelihood fits to the binned D^0 and D^+ mass distributions using the mass models and event weights as described in sections 5.1 and 5.2.

	Magnet up	Magnet down	Mean
$A_{\mathrm{raw}}(K^-\pi^+\pi^+)$	-1.969 ± 0.033	-1.672 ± 0.032	-1.827 ± 0.023
$A_{\mathrm{raw}}(\overline{K}^0\pi^+)$	-0.94 ± 0.17	-0.51 ± 0.16	-0.71 ± 0.12
$A_D(K^-\pi^+)$	-1.08 ± 0.17	-1.22 ± 0.16	-1.17 ± 0.12

Table 3. Asymmetries (in %) entering the calculation of the $K^-\pi^+$ detection asymmetry for the two magnet polarities, and for the mean value. The correction for the K^0 asymmetry is applied in the bottom row. The mean values in the last column are obtained first by taking the arithmetic average over the magnet polarities and then by taking the weighted averages of the 2011 and 2012 data sets. The uncertainties are statistical only.
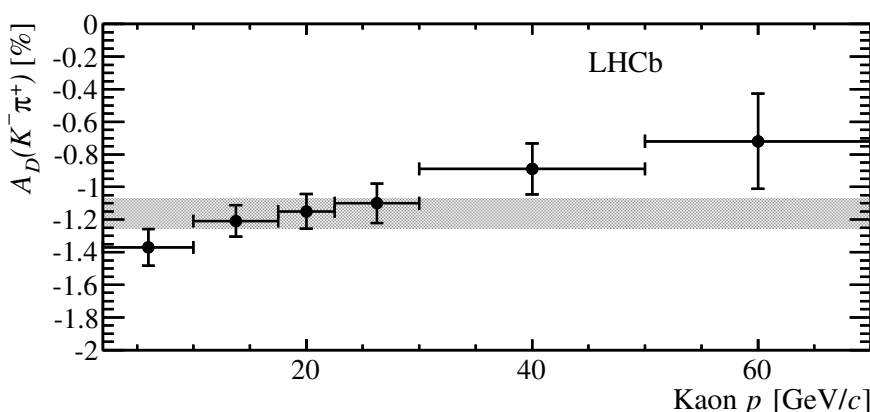

Figure 3. Measured $K^-\pi^+$ detection asymmetry as a function of the kaon momentum. The shaded band indicates the average asymmetry integrated over the bins. There is a correlation between the data points due to the overlap between the $D^+ \to \overline{K}^0\pi^+$ samples used for each bin.

The fits are done separately for the 2011 and 2012 data sets and for the two magnet polarities. For each data set the mean value of the raw asymmetry is the arithmetic average of the fit results for the two magnet polarities. The final raw asymmetry is then the statistically weighted average over the full data set. The derivation of the $K^-\pi^+$ detection asymmetry using prompt $D^+ \to K^-\pi^+\pi^+$ and $D^+ \to \overline{K}^0\pi^+$ decays is shown in table 3. The measured asymmetry, $A_D(K^-\pi^+) = (-1.17 \pm 0.12)\%$, is dominated by the different interaction cross sections of K^- and K^+ mesons in matter. Figure 3 shows the detection asymmetry as a function of the kaon momentum. As expected, the kaon interaction asymmetry decreases with kaon momentum.

For illustration, figure 4 shows the raw asymmetries for $D^0 \to K^-K^+$ and $D^0 \to \pi^-\pi^+$ candidates as functions of the invariant mass. The raw asymmetry in both decay modes is slightly negative. The derivation of ΔA_{CP} and $A_{CP}(K^-K^+)$ from the raw asymmetries are shown in tables 4 and 5. There is a statistical correlation $\rho = 0.23$ between the values of ΔA_{CP} and $A_{CP}(K^-K^+)$ as they both use candidates in the $D^0 \to K^-K^+$ sample.
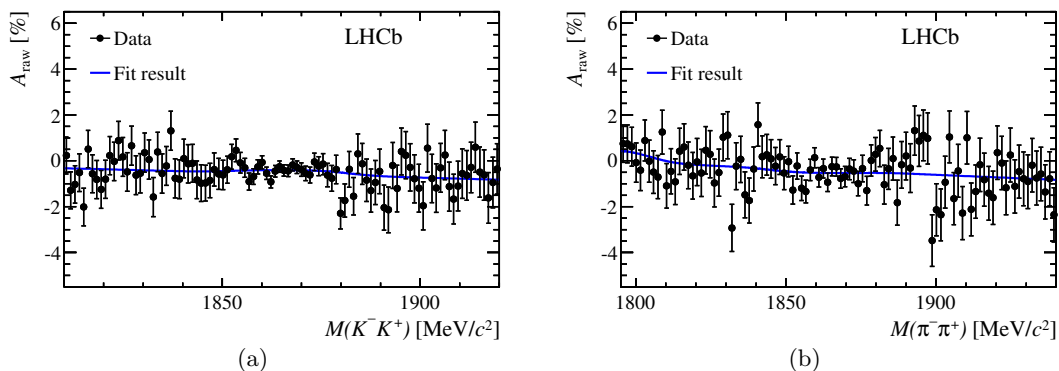
Figure 4. Raw asymmetry, without background subtraction, as a function of the invariant mass for (a) the $D^0 \to K^- K^+$ candidates and (b) the $D^0 \to \pi^- \pi^+$ candidates for the ΔA_{CP} selection. The result from the fit is overlaid.

	Magnet up	Magnet down	Mean
$A_{\mathrm{raw}}(K^- K^+)$	-0.46 ± 0.11	-0.43 ± 0.11	-0.44 ± 0.08
$A_{\mathrm{raw}}(\pi^- \pi^+)$	-0.45 ± 0.20	-0.66 ± 0.19	-0.58 ± 0.14
ΔA_{CP}	-0.01 ± 0.23	$+0.24 \pm 0.22$	$+0.14 \pm 0.16$

Table 4. Asymmetries (in %) used in the calculation of ΔA_{CP} for the two magnet polarities. The values for ΔA_{CP} are corrected for the mistag probability. The mean values in the last column are obtained first by taking the arithmetic average over the magnet polarities and then by taking the weighted averages of the 2011 and 2012 data sets. The uncertainties are statistical only.

	Magnet up	Magnet down	Mean
$A_{\mathrm{raw}}(K^- K^+)$	-0.45 ± 0.12	-0.41 ± 0.12	-0.43 ± 0.08
$A_{\mathrm{raw}}(K^- \pi^+)$	-1.41 ± 0.05	-1.59 ± 0.05	-1.51 ± 0.04
$A_D(K^- \pi^+)$	-1.08 ± 0.17	-1.22 ± 0.16	-1.17 ± 0.12
$A_{CP}(K^- K^+)$	-0.09 ± 0.21	-0.01 ± 0.21	-0.06 ± 0.15

Table 5. Asymmetries (in %) used in the calculation of $A_{CP}(K^- K^+)$ for the two magnet polarities. The values for $A_{CP}(K^- K^+)$ are corrected for the mistag probability. The mean values in the last column are obtained first by taking the arithmetic average over the magnet polarities and then by taking the weighted averages of the 2011 and 2012 data sets. The uncertainties are statistical only.

6 Systematic uncertainties

Systematic shifts in the observed CP asymmetries can arise from non-cancellation of production and detection asymmetries, misreconstruction of the final state, and imperfect modelling of the background. The contributions to the systematic uncertainties in ΔA_{CP} and $A_{CP}(K^- K^+)$ are described below.

The fractions of B^0 and B^+ decays in the three semileptonic B samples can be slightly different. Assuming that there is a difference in the B^0 and B^+ production asymmetries, a residual production asymmetry can remain in ΔA_{CP} and $A_{CP}(K^-K^+)$. As in the previous publication [11], a systematic uncertainty of 0.02% is assigned to both ΔA_{CP} and $A_{CP}(K^-K^+)$. Due to B^0 oscillations, the observed B production asymmetry depends on the decay-time acceptance of the reconstructed B meson, which is slightly different for the three decay modes. This produces a systematic uncertainty of 0.02% for both ΔA_{CP} and $A_{CP}(K^-K^+)$, similar to the one found previously [11].

The weighting procedure almost equalises the p_{T} and η distributions of the particles, but small differences remain. When also weighting for different azimuthal angle distributions of the final state particles, the change in both ΔA_{CP} and $A_{CP}(K^-K^+)$ is negligible. Slightly larger shifts are seen when increasing (decreasing) the number of bins used in each kinematic variable from 20 to 25 (15) or when changing the D^0 mass range. The maximum shift, 0.02% for ΔA_{CP} and 0.05% for $A_{CP}(K^-K^+)$, is taken as a systematic uncertainty. Finally, the cancellation of the production and detection asymmetries is tested by randomly assigning the charge of the muon or charged D meson in real data, depending on the p_{T} of the particles. The B and D^+ production asymmetries and the $\mu^\pm$, $K^\pm$ and $\pi^\pm$ detection asymmetries that are simulated in this way are motivated by the small p_{T}-dependences observed in data. No shift is seen in the value of ΔA_{CP}, while a small shift of 0.03% is observed in the value of $A_{CP}(K^-K^+)$. This shift is propagated as part of the uncertainty due the weighting procedure.

The sensitivity of the results to the signal and background models is determined by varying the signal and background functions. The alternative signal functions are a Johnson S_U distribution [31], a single Gaussian, and a double Gaussian function. The alternative background function is a second-order polynomial. Furthermore, the effect of using different mass binning and fit range, and the effect of constraining the asymmetry of the $D^0 \to K^-\pi^+$ background in the $D^0 \to \pi^-\pi^+$ decay to the observed asymmetry, are considered. The maximum variations from the default fit for each decay mode are added in quadrature to determine the systematic uncertainty for ΔA_{CP} (0.06%) and for $A_{CP}(K^-K^+)$ (0.06%).

In the default fit, the background can vary freely with an overall asymmetry and different slope parameters for each tag. Nevertheless, background contributions from different origins can have different shapes and asymmetries. Such an effect is expected to be largest in the $D^0 \to K^-K^+$ decay, due to possible contributions from other charm decays, and is studied by generating pseudoexperiments with different background compositions in the two Cabibbo-suppressed decays. Three types of background shapes are simulated: an exponential function to describe the combinatorial background observed in data, another exponential function with a different slope inspired by partially-reconstructed background from simulated $D^+ \to K^-\pi^+\pi^+$ decays, and a linear shape inspired by partially-reconstructed background from simulated $\Lambda_c^+ \to pK^-\pi^+$ decays. The asymmetries in the background are varied by up to $\pm 3\%$. Such large asymmetries are incompatible with the asymmetries observed in the background and therefore constitute an upper bound on the magnitude of any possible effect. The largest bias in the raw asymmetry (0.03%) is propagated as a systematic uncertainty for ΔA_{CP} and $A_{CP}(K^-K^+)$.

Source of uncertainty	ΔA_{CP}	$A_{CP}(K^-K^+)$
Production asymmetry:		
Difference in b-hadron mixture	0.02%	0.02%
Difference in B decay time acceptance	0.02%	0.02%
Production and detection asymmetry:		
Different weighting	0.02%	0.05%
Non-cancellation	—	0.03%
Neutral kaon asymmetry	—	0.01%
Background from real D^0 mesons:		
Mistag asymmetry	0.03%	0.03%
Background from fake D^0 mesons:		
D^0 mass fit model	0.06%	0.06%
Wrong background modelling	0.03%	0.03%
Quadratic sum	0.08%	0.10%

Table 6. Contributions to the systematic uncertainty of ΔA_{CP} and $A_{CP}(K^-K^+)$.

The systematic shift in the raw asymmetries when removing multiple candidates is below 0.005% and therefore neglected. Higher-order corrections to eq. (2.2) are at the 10^{-6} level and are neglected as well. The systematic uncertainty from the neutral kaon asymmetry (0.01%) is taken from section 5.3 and the systematic uncertainty from wrong combinations of muons and D^0 mesons is taken from section 5.4. All systematic uncertainties are summarised in table 6 for ΔA_{CP} and $A_{CP}(K^-K^+)$. The correlation coefficient between the total systematic uncertainties is $\rho = 0.40$.

7 Consistency checks

As a consistency check, the raw asymmetries in the $D^0 \to K^-K^+$ and $D^0 \to \pi^-\pi^+$ samples and ΔA_{CP} are determined as functions of the impact parameter of the D^0 trajectory with respect to the primary vertex, the flight distance of the B candidate, the angle between the directions of the muon and the D^0 decay products, the muon and D^0 kinematic variables, the reconstructed $D^0\mu$ invariant mass, the multiplicity of tracks and primary vertices in the event, the particle identification requirement on the kaons, and the selected trigger lines. No significant dependence is observed on any of these variables. Another test is made by including D^0 candidates with negative decay times. In particular in the $D^0 \to \pi^-\pi^+$ decay, there is more background at low D^0 decay times. Enhancing this type of background by including negative decay time candidates does not change the values for ΔA_{CP} or $A_{CP}(K^-K^+)$.

During periods without data taking, interventions on the detector and on the trigger change the alignment and data acquisition conditions. This could induce time-varying
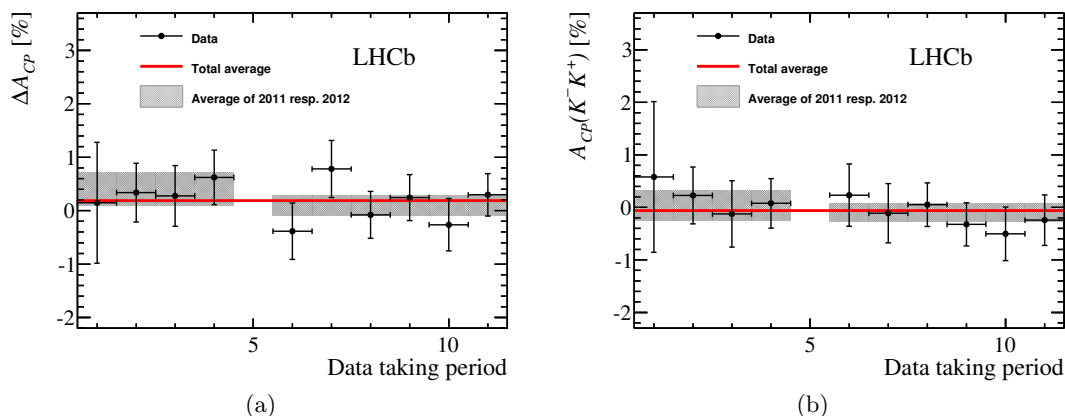
Figure 5. (a) ΔA_{CP} and (b) $A_{CP}(K^-K^+)$ as a function of the data taking period. The 2011 data are divided into four periods and the 2012 data into six periods. The error bars indicate the statistical uncertainty, the shaded bands show the averages for 2011 and 2012, and the (red) line shows the overall CP asymmetry.

detection asymmetries. The final results should not be sensitive to such variations as data are calibrated with control samples collected in the same data-taking period. Nevertheless, any residual detector asymmetry would manifest itself as variations in time of the measured CP asymmetries. Figure 5 shows ΔA_{CP} and $A_{CP}(K^-K^+)$ versus data taking period. These periods are separated by interruptions in data taking, and within each period the magnetic field is reversed at least once. No dependence of the obtained CP asymmetries on the data taking period is observed. The average values of ΔA_{CP} are $(+0.33 \pm 0.30\,(\mathrm{stat}))\%$ for the 2011 data and $(+0.06 \pm 0.19\,(\mathrm{stat}))\%$ for the 2012 data. The value for the 2011 data is slightly lower compared to the previous analysis, which is attributed to the non-overlapping data samples, due to differences in the selection and in the calibration of the detector. The main shift is due to the looser particle identification requirements on the kaons in this analysis. Such a shift is not seen in the 2012 data. The average values of $A_{CP}(K^-K^+)$ are $(+0.04 \pm 0.28\,(\mathrm{stat}))\%$ for the 2011 data and $(-0.10 \pm 0.18\,(\mathrm{stat}))\%$ for the 2012 data.

8 Conclusion

The difference in CP asymmetries between the $D^0 \to K^-K^+$ and $D^0 \to \pi^-\pi^+$ decay channels and the CP asymmetry in the $D^0 \to K^-K^+$ channel are measured using muon-tagged D^0 decays in the $3\,\mathrm{fb}^{-1}$ data set to be

$$\Delta A_{CP} = (+0.14 \pm 0.16\,(\mathrm{stat}) \pm 0.08\,(\mathrm{syst}))\%\,,$$
$$A_{CP}(K^-K^+) = (-0.06 \pm 0.15\,(\mathrm{stat}) \pm 0.10\,(\mathrm{syst}))\%\,,$$

where the total correlation coefficient, including statistical and systematic components, is $\rho = 0.28$. By combining the above results, the CP asymmetry in the $D^0 \to \pi^-\pi^+$ decay is found to be

$$A_{CP}(\pi^-\pi^+) = (-0.20 \pm 0.19\,(\mathrm{stat}) \pm 0.10\,(\mathrm{syst}))\%\,.$$

These results are obtained assuming that there is no CP violation in D^0 mixing and no direct CP violation in the Cabibbo-favoured $D^0 \to K^- \pi^+$, $D^+ \to K^- \pi^+ \pi^+$ and $D^+ \to \overline{K}^0 \pi^+$ decay modes. The measurement of ΔA_{CP} supersedes the previously reported result [11]. Our results show that there is no significant CP violation in the singly Cabibbo-suppressed $D^0 \to K^- K^+, \pi^- \pi^+$ decays at the level of 10^{-3}. These results constitute the most precise measurements of time-integrated CP asymmetries $A_{CP}(K^- K^+)$ and $A_{CP}(\pi^- \pi^+)$ from a single experiment to date.

Acknowledgments

References

[1] M. Bobrowski, A. Lenz, J. Riedl and J. Rohrwild, *How large can the SM contribution to CP-violation in D^0-$\bar{D}^0$ mixing be?*, *JHEP* **03** (2010) 009 [arXiv:1002.4794] [ɪɴSPIRE].

[2] Y. Grossman, A.L. Kagan and Y. Nir, *New physics and CP-violation in singly Cabibbo suppressed D decays*, *Phys. Rev.* **D 75** (2007) 036008 [hep-ph/0609178] [ɪɴSPIRE].

[3] T. Feldmann, S. Nandi and A. Soni, *Repercussions of flavour symmetry breaking on CP-violation in D-meson decays*, *JHEP* **06** (2012) 007 [arXiv:1202.3795] [ɪɴSPIRE].

[4] J. Brod, A.L. Kagan and J. Zupan, *Size of direct CP-violation in singly Cabibbo-suppressed D decays*, *Phys. Rev.* **D 86** (2012) 014023 [arXiv:1111.5000] [ɪɴSPIRE].

[5] B. Bhattacharya, M. Gronau and J.L. Rosner, *CP asymmetries in singly-Cabibbo-suppressed D decays to two pseudoscalar mesons*, *Phys. Rev.* **D 85** (2012) 054014 [arXiv:1201.2351] [ɪɴSPIRE].

[6] LHCb collaboration, *Implications of LHCb measurements and future prospects*, *Eur. Phys. J.* **C 73** (2013) 2373 [arXiv:1208.3355] [InSPIRE].

[7] S. Bianco, F.L. Fabbri, D. Benson and I. Bigi, *A Cicerone for the physics of charm*, *Riv. Nuovo Cim.* **26N7** (2003) 1 [hep-ex/0309021] [InSPIRE].

[8] HEAVY FLAVOR AVERAGING GROUP collaboration, Y. Amhis et al., *Averages of B-hadron, C-hadron and τ-lepton properties as of early 2012*, arXiv:1207.1158 [InSPIRE].

[9] LHCb collaboration, *Evidence for CP-violation in time-integrated $D^0 \to h^- h^+$ decay rates*, *Phys. Rev. Lett.* **108** (2012) 111602 [arXiv:1112.0938] [InSPIRE].

[10] LHCb Collaboration, *A search for time-integrated CP-violation in $D^0 \to K^- K^+$ and $D^0 \to \pi^- \pi^+$ decays*, LHCb-CONF-2013-003 (2013).

[11] LHCb collaboration, *Search for direct CP violation in $D^0 \to h^- h^+$ modes using semileptonic B decays*, *Phys. Lett.* **B 723** (2013) 33 [arXiv:1303.2614] [InSPIRE].

[12] BABAR collaboration, B. Aubert et al., *Search for CP-violation in the decays $D^0 \to K^- K^+$ and $D^0 \to \pi^- \pi^+$*, *Phys. Rev. Lett.* **100** (2008) 061803 [arXiv:0709.2715] [InSPIRE].

[13] CDF collaboration, T. Aaltonen et al., *Measurement of CP-violating asymmetries in $D^0 \to \pi^+ \pi^-$ and $D^0 \to K^+ K^-$ decays at CDF*, *Phys. Rev.* **D 85** (2012) 012009 [arXiv:1111.5023] [InSPIRE].

[14] CDF collaboration, T. Aaltonen et al., *Measurement of the difference of CP-violating asymmetries in $D^0 \to K^+ K^-$ and $D^0 \to \pi^+ \pi^-$ decays at CDF*, *Phys. Rev. Lett.* **109** (2012) 111801 [arXiv:1207.2158] [InSPIRE].

[15] BELLE collaboration, M. Staric et al., *Measurement of CP asymmetry in Cabibbo suppressed D^0 decays*, *Phys. Lett.* **B 670** (2008) 190 [arXiv:0807.0148] [InSPIRE].

[16] BELLE collaboration, B.R. Ko, *Direct CP-violation in charm at Belle*, PoS(ICHEP2012)353 [arXiv:1212.1975] [InSPIRE].

[17] LHCb collaboration, *The LHCb detector at the LHC*, 2008 *JINST* **3** S08005 [InSPIRE].

[18] M. Adinolfi et al., *Performance of the LHCb RICH detector at the LHC*, *Eur. Phys. J.* **C 73** (2013) 2431 [arXiv:1211.6759] [InSPIRE].

[19] R. Aaij et al., *The LHCb trigger and its performance in 2011*, 2013 *JINST* **8** P04022 [arXiv:1211.3055] [InSPIRE].

[20] W.D. Hulsbergen, *Decay chain fitting with a Kalman filter*, *Nucl. Instrum. Meth.* **A 552** (2005) 566 [physics/0503191] [InSPIRE].

[21] PARTICLE DATA GROUP collaboration, J. Beringer et al., *Review of particle physics*, *Phys. Rev.* **D 86** (2012) 010001 [InSPIRE].

[22] LHCb collaboration, *Precision measurement of D meson mass differences*, *JHEP* **06** (2013) 065 [arXiv:1304.6865] [InSPIRE].

[23] A. Pais and O. Piccioni, *Note on the decay and absorption of the θ^0*, *Phys. Rev.* **100** (1955) 1487 [InSPIRE].

[24] W. Fetscher, P. Kokkas, P. Pavlopoulos, T. Schietinger and T. Ruf, *Regeneration of arbitrary coherent neutral kaon states: a new method for measuring the $K^0 \bar{K}^0$ forward scattering amplitude*, *Z. Phys.* **C 72** (1996) 543 [InSPIRE].

[25] A. Gsponer, J. Hoffnagle, W.R. Molzon, J. Roehrig, V.L. Telegdi et al., *Precise coherent K_S regeneration amplitudes for C, Al, Cu, SN and Pb nuclei from 20 GeV/c to 140 GeV/c and their interpretation*, *Phys. Rev. Lett.* **42** (1979) 13 [INSPIRE].

[26] R.A. Briere and B. Winstein, *Determining the phase of a strong scattering amplitude from its momentum dependence to better than 1-degree: the example of kaon regeneration*, *Phys. Rev. Lett.* **75** (1995) 402 [*Erratum ibid.* **75** (1995) 2070] [INSPIRE].

[27] M.L. Good, *Relation between scattering and absorption in the Pais-Piccioni phenomenon*, *Phys. Rev.* **106** (1957) 591 [INSPIRE].

[28] LHCb collaboration, *Measurement of the $D^\pm$ production asymmetry in 7 TeV pp collisions*, *Phys. Lett.* **B 718** (2013) 902 [arXiv:1210.4112] [INSPIRE].

[29] LHCb collaboration, *Measurement of D^0-$\bar{D}^0$ mixing parameters and search for CP-violation using $D^0 \to K^+\pi^-$ decays*, *Phys. Rev. Lett.* **111** (2013) 251801 [arXiv:1309.6534] [INSPIRE].

[30] M. Pivk and F.R. Le Diberder, *SPlot: a statistical tool to unfold data distributions*, *Nucl. Instrum. Meth.* **A 555** (2005) 356 [physics/0402083] [INSPIRE].

[31] N. Johnson, *Systems of frequency curves generated by methods of translation*, *Biometrika* **36** (1949) 149.

The LHCb collaboration

R. Aaij[41], B. Adeva[37], M. Adinolfi[46], A. Affolder[52], Z. Ajaltouni[5], J. Albrecht[9], F. Alessio[38], M. Alexander[51], S. Ali[41], G. Alkhazov[30], P. Alvarez Cartelle[37], A.A. Alves Jr[25,38], S. Amato[2], S. Amerio[22], Y. Amhis[7], L. An[3], L. Anderlini[17,g], J. Anderson[40], R. Andreassen[57], M. Andreotti[16,f], J.E. Andrews[58], R.B. Appleby[54], O. Aquines Gutierrez[10], F. Archilli[38], A. Artamonov[35], M. Artuso[59], E. Aslanides[6], G. Auriemma[25,n], M. Baalouch[5], S. Bachmann[11], J.J. Back[48], A. Badalov[36], V. Balagura[31], W. Baldini[16], R.J. Barlow[54], C. Barschel[38], S. Barsuk[7], W. Barter[47], V. Batozskaya[28], Th. Bauer[41], A. Bay[39], L. Beaucourt[4], J. Beddow[51], F. Bedeschi[23], I. Bediaga[1], S. Belogurov[31], K. Belous[35], I. Belyaev[31], E. Ben-Haim[8], G. Bencivenni[18], S. Benson[38], J. Benton[46], A. Berezhnoy[32], R. Bernet[40], M.-O. Bettler[47], M. van Beuzekom[41], A. Bien[11], S. Bifani[45], T. Bird[54], A. Bizzeti[17,i], P.M. Bjørnstad[54], T. Blake[48], F. Blanc[39], J. Blouw[10], S. Blusk[59], V. Bocci[25], A. Bondar[34], N. Bondar[30,38], W. Bonivento[15,38], S. Borghi[54], A. Borgia[59], M. Borsato[7], T.J.V. Bowcock[52], E. Bowen[40], C. Bozzi[16], T. Brambach[9], J. van den Brand[42], J. Bressieux[39], D. Brett[54], M. Britsch[10], T. Britton[59], J. Brodzicka[54], N.H. Brook[46], H. Brown[52], A. Bursche[40], G. Busetto[22,q], J. Buytaert[38], S. Cadeddu[15], R. Calabrese[16,f], M. Calvi[20,k], M. Calvo Gomez[36,o], A. Camboni[36], P. Campana[18,38], D. Campora Perez[38], A. Carbone[14,d], G. Carboni[24,l], R. Cardinale[19,38,j], A. Cardini[15], H. Carranza-Mejia[50], L. Carson[50], K. Carvalho Akiba[2], G. Casse[52], L. Cassina[20], L. Castillo Garcia[38], M. Cattaneo[38], Ch. Cauet[9], R. Cenci[58], M. Charles[8], Ph. Charpentier[38], S. Chen[54], S.-F. Cheung[55], N. Chiapolini[40], M. Chrzaszcz[40,26], K. Ciba[38], X. Cid Vidal[38], G. Ciezarek[53], P.E.L. Clarke[50], M. Clemencic[38], H.V. Cliff[47], J. Closier[38], V. Coco[38], J. Cogan[6], E. Cogneras[5], P. Collins[38], A. Comerma-Montells[11], A. Contu[15,38], A. Cook[46], M. Coombes[46], S. Coquereau[8], G. Corti[38], M. Corvo[16,f], I. Counts[56], B. Couturier[38], G.A. Cowan[50], D.C. Craik[48], M. Cruz Torres[60], S. Cunliffe[53], R. Currie[50], C. D'Ambrosio[38], J. Dalseno[46], P. David[8], P.N.Y. David[41], A. Davis[57], K. De Bruyn[41], S. De Capua[54], M. De Cian[11], J.M. De Miranda[1], L. De Paula[2], W. De Silva[57], P. De Simone[18], D. Decamp[4], M. Deckenhoff[9], L. Del Buono[8], N. Déléage[4], D. Derkach[55], O. Deschamps[5], F. Dettori[42], A. Di Canto[38], H. Dijkstra[38], S. Donleavy[52], F. Dordei[11], M. Dorigo[39], A. Dosil Suárez[37], D. Dossett[48], A. Dovbnya[43], G. Dujany[54], F. Dupertuis[39], P. Durante[38], R. Dzhelyadin[35], A. Dziurda[26], A. Dzyuba[30], S. Easo[49,38], U. Egede[53], V. Egorychev[31], S. Eidelman[34], S. Eisenhardt[50], U. Eitschberger[9], R. Ekelhof[9], L. Eklund[51,38], I. El Rifai[5], Ch. Elsasser[40], S. Ely[59], S. Esen[11], T. Evans[55], A. Falabella[16,f], C. Färber[11], C. Farinelli[41], N. Farley[45], S. Farry[52], D. Ferguson[50], V. Fernandez Albor[37], F. Ferreira Rodrigues[1], M. Ferro-Luzzi[38], S. Filippov[33], M. Fiore[16,f], M. Fiorini[16,f], M. Firlej[27], C. Fitzpatrick[38], T. Fiutowski[27], M. Fontana[10], F. Fontanelli[19,j], R. Forty[38], O. Francisco[2], M. Frank[38], C. Frei[38], M. Frosini[17,38,g], J. Fu[21,38], E. Furfaro[24,l], A. Gallas Torreira[37], D. Galli[14,d], S. Gallorini[22], S. Gambetta[19,j], M. Gandelman[2], P. Gandini[59], Y. Gao[3], J. Garofoli[59], J. Garra Tico[47], L. Garrido[36], C. Gaspar[38], R. Gauld[55], L. Gavardi[9], E. Gersabeck[11], M. Gersabeck[54], T. Gershon[48], Ph. Ghez[4], A. Gianelle[22], S. Giani'[39], V. Gibson[47], L. Giubega[29], V.V. Gligorov[38], C. Göbel[60], D. Golubkov[31], A. Golutvin[53,31,38], A. Gomes[1,a], H. Gordon[38], C. Gotti[20], M. Grabalosa Gándara[5], R. Graciani Diaz[36], L.A. Granado Cardoso[38], E. Graugés[36], G. Graziani[17], A. Grecu[29], E. Greening[55], S. Gregson[47], P. Griffith[45], L. Grillo[11], O. Grünberg[62], B. Gui[59], E. Gushchin[33], Yu. Guz[35,38], T. Gys[38], C. Hadjivasiliou[59], G. Haefeli[39], C. Haen[38], S.C. Haines[47], S. Hall[53], B. Hamilton[58], T. Hampson[46], X. Han[11], S. Hansmann-Menzemer[11], N. Harnew[55], S.T. Harnew[46], J. Harrison[54], T. Hartmann[62], J. He[38], T. Head[38], V. Heijne[41], K. Hennessy[52], P. Henrard[5], L. Henry[8], J.A. Hernando Morata[37], E. van Herwijnen[38], M. Heß[62], A. Hicheur[1], D. Hill[55], M. Hoballah[5], C. Hombach[54], W. Hulsbergen[41], P. Hunt[55], N. Hussain[55], D. Hutchcroft[52], D. Hynds[51],

– 20 –

M. Idzik[27], P. Ilten[56], R. Jacobsson[38], A. Jaeger[11], J. Jalocha[55], E. Jans[41], P. Jaton[39],
A. Jawahery[58], M. Jezabek[26], F. Jing[3], M. John[55], D. Johnson[55], C.R. Jones[47], C. Joram[38],
B. Jost[38], N. Jurik[59], M. Kaballo[9], S. Kandybei[43], W. Kanso[6], M. Karacson[38], T.M. Karbach[38],
M. Kelsey[59], I.R. Kenyon[45], T. Ketel[42], B. Khanji[20], C. Khurewathanakul[39], S. Klaver[54],
O. Kochebina[7], M. Kolpin[11], I. Komarov[39], R.F. Koopman[42], P. Koppenburg[41,38], M. Korolev[32],
A. Kozlinskiy[41], L. Kravchuk[33], K. Kreplin[11], M. Kreps[48], G. Krocker[11], P. Krokovny[34],
F. Kruse[9], M. Kucharczyk[20,26,38,k], V. Kudryavtsev[34], K. Kurek[28], T. Kvaratskheliya[31],
V.N. La Thi[39], D. Lacarrere[38], G. Lafferty[54], A. Lai[15], D. Lambert[50], R.W. Lambert[42],
E. Lanciotti[38], G. Lanfranchi[18], C. Langenbruch[38], B. Langhans[38], T. Latham[48], C. Lazzeroni[45],
R. Le Gac[6], J. van Leerdam[41], J.-P. Lees[4], R. Lefèvre[5], A. Leflat[32], J. Lefrançois[7], S. Leo[23],
O. Leroy[6], T. Lesiak[26], B. Leverington[11], Y. Li[3], M. Liles[52], R. Lindner[38], C. Linn[38],
F. Lionetto[40], B. Liu[15], G. Liu[38], S. Lohn[38], I. Longstaff[51], J.H. Lopes[2], N. Lopez-March[39],
P. Lowdon[40], H. Lu[3], D. Lucchesi[22,q], H. Luo[50], A. Lupato[22], E. Luppi[16,f], O. Lupton[55],
F. Machefert[7], I.V. Machikhiliyan[31], F. Maciuc[29], O. Maev[30], S. Malde[55], G. Manca[15,e],
G. Mancinelli[6], M. Manzali[16,f], J. Maratas[5], J.F. Marchand[4], U. Marconi[14], C. Marin Benito[36],
P. Marino[23,s], R. Märki[39], J. Marks[11], G. Martellotti[25], A. Martens[8], A. Martín Sánchez[7],
M. Martinelli[41], D. Martinez Santos[42], F. Martinez Vidal[64], D. Martins Tostes[2], A. Massafferri[1],
R. Matev[38], Z. Mathe[38], C. Matteuzzi[20], A. Mazurov[16,f], M. McCann[53], J. McCarthy[45],
A. McNab[54], R. McNulty[12], B. McSkelly[52], B. Meadows[57,55], F. Meier[9], M. Meissner[11],
M. Merk[41], D.A. Milanes[8], M.-N. Minard[4], N. Moggi[14], J. Molina Rodriguez[60], S. Monteil[5],
D. Moran[54], M. Morandin[22], P. Morawski[26], A. Mordà[6], M.J. Morello[23,s], J. Moron[27],
A.-B. Morris[50], R. Mountain[59], F. Muheim[50], K. Müller[40], R. Muresan[29], M. Mussini[14],
B. Muster[39], P. Naik[46], T. Nakada[39], R. Nandakumar[49], I. Nasteva[2], M. Needham[50], N. Neri[21],
S. Neubert[38], N. Neufeld[38], M. Neuner[11], A.D. Nguyen[39], T.D. Nguyen[39], C. Nguyen-Mau[39,p],
M. Nicol[7], V. Niess[5], R. Niet[9], N. Nikitin[32], T. Nikodem[11], A. Novoselov[35],
A. Oblakowska-Mucha[27], V. Obraztsov[35], S. Oggero[41], S. Ogilvy[51], O. Okhrimenko[44],
R. Oldeman[15,e], G. Onderwater[65], M. Orlandea[29], J.M. Otalora Goicochea[2], P. Owen[53],
A. Oyanguren[64], B.K. Pal[59], A. Palano[13,c], F. Palombo[21,t], M. Palutan[18], J. Panman[38],
A. Papanestis[49,38], M. Pappagallo[51], C. Parkes[54], C.J. Parkinson[9], G. Passaleva[17], G.D. Patel[52],
M. Patel[53], C. Patrignani[19,j], A. Pazos Alvarez[37], A. Pearce[54], A. Pellegrino[41],
M. Pepe Altarelli[38], S. Perazzini[14,d], E. Perez Trigo[37], P. Perret[5], M. Perrin-Terrin[6],
L. Pescatore[45], E. Pesen[66], K. Petridis[53], A. Petrolini[19,j], E. Picatoste Olloqui[36], B. Pietrzyk[4],
T. Pilař[48], D. Pinci[25], A. Pistone[19], S. Playfer[50], M. Plo Casasus[37], F. Polci[8], A. Poluektov[48,34],
E. Polycarpo[2], A. Popov[35], D. Popov[10], B. Popovici[29], C. Potterat[2], A. Powell[55],
J. Prisciandaro[39], A. Pritchard[52], C. Prouve[46], V. Pugatch[44], A. Puig Navarro[39], G. Punzi[23,r],
W. Qian[4], B. Rachwal[26], J.H. Rademacker[46], B. Rakotomiaramanana[39], M. Rama[18],
M.S. Rangel[2], I. Raniuk[43], N. Rauschmayr[38], G. Raven[42], S. Reichert[54], M.M. Reid[48],
A.C. dos Reis[1], S. Ricciardi[49], A. Richards[53], M. Rihl[38], K. Rinnert[52], V. Rives Molina[36],
D.A. Roa Romero[5], P. Robbe[7], A.B. Rodrigues[1], E. Rodrigues[54], P. Rodriguez Perez[54],
S. Roiser[38], V. Romanovsky[35], A. Romero Vidal[37], M. Rotondo[22], J. Rouvinet[39], T. Ruf[38],
F. Ruffini[23], H. Ruiz[36], P. Ruiz Valls[64], G. Sabatino[25,l], J.J. Saborido Silva[37], N. Sagidova[30],
P. Sail[51], B. Saitta[15,e], V. Salustino Guimaraes[2], C. Sanchez Mayordomo[64], B. Sanmartin Sedes[37],
R. Santacesaria[25], C. Santamarina Rios[37], E. Santovetti[24,l], A. Sapunov[6], A. Sarti[18,m],
C. Satriano[25,n], A. Satta[24], M. Savrie[16,f], D. Savrina[31,32], M. Schiller[42], H. Schindler[38],
M. Schlupp[9], M. Schmelling[10], B. Schmidt[38], O. Schneider[39], A. Schopper[38], M.-H. Schune[7],
R. Schwemmer[38], B. Sciascia[18], A. Sciubba[25], M. Seco[37], A. Semennikov[31], K. Senderowska[27],
I. Sepp[53], N. Serra[40], J. Serrano[6], L. Sestini[22], P. Seyfert[11], M. Shapkin[35], I. Shapoval[16,43,f],
Y. Shcheglov[30], T. Shears[52], L. Shekhtman[34], V. Shevchenko[63], A. Shires[9], R. Silva Coutinho[48],

G. Simi[22], M. Sirendi[47], N. Skidmore[46], T. Skwarnicki[59], N.A. Smith[52], E. Smith[55,49], E. Smith[53], J. Smith[47], M. Smith[54], H. Snoek[41], M.D. Sokoloff[57], F.J.P. Soler[51], F. Soomro[39], D. Souza[46], B. Souza De Paula[2], B. Spaan[9], A. Sparkes[50], F. Spinella[23], P. Spradlin[51], F. Stagni[38], S. Stahl[11], O. Steinkamp[40], O. Stenyakin[35], S. Stevenson[55], S. Stoica[29], S. Stone[59], B. Storaci[40], S. Stracka[23,38], M. Straticiuc[29], U. Straumann[40], R. Stroili[22], V.K. Subbiah[38], L. Sun[57], W. Sutcliffe[53], K. Swientek[27], S. Swientek[9], V. Syropoulos[42], M. Szczekowski[28], P. Szczypka[39,38], D. Szilard[2], T. Szumlak[27], S. T'Jampens[4], M. Teklishyn[7], G. Tellarini[16,f], F. Teubert[38], C. Thomas[55], E. Thomas[38], J. van Tilburg[41], V. Tisserand[4], M. Tobin[39], S. Tolk[42], L. Tomassetti[16,f], D. Tonelli[38], S. Topp-Joergensen[55], N. Torr[55], E. Tournefier[4], S. Tourneur[39], M.T. Tran[39], M. Tresch[40], A. Tsaregorodtsev[6], P. Tsopelas[41], N. Tuning[41], M. Ubeda Garcia[38], A. Ukleja[28], A. Ustyuzhanin[63], U. Uwer[11], V. Vagnoni[14], G. Valenti[14], A. Vallier[7], R. Vazquez Gomez[18], P. Vazquez Regueiro[37], C. Vázquez Sierra[37], S. Vecchi[16], J.J. Velthuis[46], M. Veltri[17,h], G. Veneziano[39], M. Vesterinen[11], B. Viaud[7], D. Vieira[2], M. Vieites Diaz[37], X. Vilasis-Cardona[36,o], A. Vollhardt[40], D. Volyanskyy[10], D. Voong[46], A. Vorobyev[30], V. Vorobyev[34], C. Voß[62], H. Voss[10], J.A. de Vries[41], R. Waldi[62], C. Wallace[48], R. Wallace[12], J. Walsh[23], S. Wandernoth[11], J. Wang[59], D.R. Ward[47], N.K. Watson[45], D. Websdale[53], M. Whitehead[48], J. Wicht[38], D. Wiedner[11], G. Wilkinson[55], M.P. Williams[45], M. Williams[56], F.F. Wilson[49], J. Wimberley[58], J. Wishahi[9], W. Wislicki[28], M. Witek[26], G. Wormser[7], S.A. Wotton[47], S. Wright[47], S. Wu[3], K. Wyllie[38], Y. Xie[61], Z. Xing[59], Z. Xu[39], Z. Yang[3], X. Yuan[3], O. Yushchenko[35], M. Zangoli[14], M. Zavertyaev[10,b], F. Zhang[3], L. Zhang[59], W.C. Zhang[12], Y. Zhang[3], A. Zhelezov[11], A. Zhokhov[31], L. Zhong[3], A. Zvyagin[38]

1   Centro Brasileiro de Pesquisas Físicas (CBPF), Rio de Janeiro, Brazil
2   Universidade Federal do Rio de Janeiro (UFRJ), Rio de Janeiro, Brazil
3   Center for High Energy Physics, Tsinghua University, Beijing, China
4   LAPP, Université de Savoie, CNRS/IN2P3, Annecy-Le-Vieux, France
5   Clermont Université, Université Blaise Pascal, CNRS/IN2P3, LPC, Clermont-Ferrand, France
6   CPPM, Aix-Marseille Université, CNRS/IN2P3, Marseille, France
7   LAL, Université Paris-Sud, CNRS/IN2P3, Orsay, France
8   LPNHE, Université Pierre et Marie Curie, Université Paris Diderot, CNRS/IN2P3, Paris, France
9   Fakultät Physik, Technische Universität Dortmund, Dortmund, Germany
10 Max-Planck-Institut für Kernphysik (MPIK), Heidelberg, Germany
11 Physikalisches Institut, Ruprecht-Karls-Universität Heidelberg, Heidelberg, Germany
12 School of Physics, University College Dublin, Dublin, Ireland
13 Sezione INFN di Bari, Bari, Italy
14 Sezione INFN di Bologna, Bologna, Italy
15 Sezione INFN di Cagliari, Cagliari, Italy
16 Sezione INFN di Ferrara, Ferrara, Italy
17 Sezione INFN di Firenze, Firenze, Italy
18 Laboratori Nazionali dell'INFN di Frascati, Frascati, Italy
19 Sezione INFN di Genova, Genova, Italy
20 Sezione INFN di Milano Bicocca, Milano, Italy
21 Sezione INFN di Milano, Milano, Italy
22 Sezione INFN di Padova, Padova, Italy
23 Sezione INFN di Pisa, Pisa, Italy
24 Sezione INFN di Roma Tor Vergata, Roma, Italy
25 Sezione INFN di Roma La Sapienza, Roma, Italy
26 Henryk Niewodniczanski Institute of Nuclear Physics Polish Academy of Sciences, Kraków, Poland
27 AGH - University of Science and Technology, Faculty of Physics and Applied Computer Science, Kraków, Poland
28 National Center for Nuclear Research (NCBJ), Warsaw, Poland

29   *Horia Hulubei National Institute of Physics and Nuclear Engineering, Bucharest-Magurele, Romania*

30   *Petersburg Nuclear Physics Institute (PNPI), Gatchina, Russia*

31   *Institute of Theoretical and Experimental Physics (ITEP), Moscow, Russia*

32   *Institute of Nuclear Physics, Moscow State University (SINP MSU), Moscow, Russia*

33   *Institute for Nuclear Research of the Russian Academy of Sciences (INR RAN), Moscow, Russia*

34   *Budker Institute of Nuclear Physics (SB RAS) and Novosibirsk State University, Novosibirsk, Russia*

35   *Institute for High Energy Physics (IHEP), Protvino, Russia*

36   *Universitat de Barcelona, Barcelona, Spain*

37   *Universidad de Santiago de Compostela, Santiago de Compostela, Spain*

38   *European Organization for Nuclear Research (CERN), Geneva, Switzerland*

39   *Ecole Polytechnique Fédérale de Lausanne (EPFL), Lausanne, Switzerland*

40   *Physik-Institut, Universität Zürich, Zürich, Switzerland*

41   *Nikhef National Institute for Subatomic Physics, Amsterdam, The Netherlands*

42   *Nikhef National Institute for Subatomic Physics and VU University Amsterdam, Amsterdam, The Netherlands*

43   *NSC Kharkiv Institute of Physics and Technology (NSC KIPT), Kharkiv, Ukraine*

44   *Institute for Nuclear Research of the National Academy of Sciences (KINR), Kyiv, Ukraine*

45   *University of Birmingham, Birmingham, United Kingdom*

46   *H.H. Wills Physics Laboratory, University of Bristol, Bristol, United Kingdom*

47   *Cavendish Laboratory, University of Cambridge, Cambridge, United Kingdom*

48   *Department of Physics, University of Warwick, Coventry, United Kingdom*

49   *STFC Rutherford Appleton Laboratory, Didcot, United Kingdom*

50   *School of Physics and Astronomy, University of Edinburgh, Edinburgh, United Kingdom*

51   *School of Physics and Astronomy, University of Glasgow, Glasgow, United Kingdom*

52   *Oliver Lodge Laboratory, University of Liverpool, Liverpool, United Kingdom*

53   *Imperial College London, London, United Kingdom*

54   *School of Physics and Astronomy, University of Manchester, Manchester, United Kingdom*

55   *Department of Physics, University of Oxford, Oxford, United Kingdom*

56   *Massachusetts Institute of Technology, Cambridge, MA, United States*

57   *University of Cincinnati, Cincinnati, OH, United States*

58   *University of Maryland, College Park, MD, United States*

59   *Syracuse University, Syracuse, NY, United States*

60   *Pontifícia Universidade Católica do Rio de Janeiro (PUC-Rio), Rio de Janeiro, Brazil, associated to[2]*

61   *Institute of Particle Physics, Central China Normal University, Wuhan, Hubei, China, associated to[3]*

62   *Institut für Physik, Universität Rostock, Rostock, Germany, associated to[11]*

63   *National Research Centre Kurchatov Institute, Moscow, Russia, associated to[31]*

64   *Instituto de Fisica Corpuscular (IFIC), Universitat de Valencia-CSIC, Valencia, Spain, associated to[36]*

65   *KVI - University of Groningen, Groningen, The Netherlands, associated to[41]*

66   *Celal Bayar University, Manisa, Turkey, associated to[38]*

[a]   *Universidade Federal do Triângulo Mineiro (UFTM), Uberaba-MG, Brazil*

[b]   *P.N. Lebedev Physical Institute, Russian Academy of Science (LPI RAS), Moscow, Russia*

[c]   *Università di Bari, Bari, Italy*

[d]   *Università di Bologna, Bologna, Italy*

[e]   *Università di Cagliari, Cagliari, Italy*

[f]   *Università di Ferrara, Ferrara, Italy*

[g]   *Università di Firenze, Firenze, Italy*

^{h} Università di Urbino, Urbino, Italy

^{i} Università di Modena e Reggio Emilia, Modena, Italy

^{j} Università di Genova, Genova, Italy

^{k} Università di Milano Bicocca, Milano, Italy

^{l} Università di Roma Tor Vergata, Roma, Italy

^{m} Università di Roma La Sapienza, Roma, Italy

^{n} Università della Basilicata, Potenza, Italy

^{o} LIFAELS, La Salle, Universitat Ramon Llull, Barcelona, Spain

^{p} Hanoi University of Science, Hanoi, Viet Nam

^{q} Università di Padova, Padova, Italy

^{r} Università di Pisa, Pisa, Italy

^{s} Scuola Normale Superiore, Pisa, Italy

^{t} Università degli Studi di Milano, Milano, Italy